

# Synoptic-scale intraseasonal variation and its effect on interannual variation in precipitation over the middle-lower reaches of the Yellow River basin.

Hatsuki Fujinami (HyARC, Nagoya University)

## 1. Introduction.

The Yellow River is an important water source for people who live in the basin. Recently, The decrease in the water source becomes a serious problem in the area. The interannual variation in precipitation over the Yellow River basin is a main factor for inducing the flow fluctuation of the Yellow River. In the basin, the summertime (June – September) precipitation account for more than 60% of annual precipitation (e.g. Yatagai and Yasunari 1995). Therefore, the interannual variation in summertime precipitation and a factor for inducing the variation are important issues. In this study, the long-term trend and interannual variation in summertime precipitation over the Yellow River basin is examined. In addition, intraseasonal variation and its effect on the interannual variation are also discussed.

## 2. Data

Daily gridded ( $0.5^\circ$  latitude–longitude grid) precipitation data made by Xie et al (2007) is used in this study. This data was made using many gauge observations over China, including the daily gauge data from the Chinese Yellow River Conservation Commission over the Yellow River basin. The data is available for the period from 1978 to 2002. GPCP (Global Precipitation Climatology Project; Huffman et al., 1997) data is also used to investigate precipitation variability in broader area for longer period. The data has global coverage on  $2.5^\circ$  latitude–longitude grid. The data is used from 1979 to 2006. Daily averaged National Center for Environmental Prediction (NCEP)/National Center for Atmospheric Research (NCAR) reanalysis data represent the large-scale circulation. The data are defined on global  $2.5^\circ \times 2.5^\circ$  grids (Kalnay et al. 1996).

## 3. Results

### 3.1 Interannual variation in precipitation over the Yellow River basin during the summer

In this study, the Yellow River basin is defined as the grid box of  $34^\circ - 43^\circ\text{N}$ ,  $105^\circ - 120^\circ\text{E}$ , which contains the middle – lower reaches of the Yellow River (the Loess Plateau to the mouth of the Yellow River). Figure 1 shows the time-latitude section in the climatological seasonal march of precipitation in the longitudes of the Yellow River basin. A precipitation maximum from mid-June to mid-July over the Yangtze River basin ( $30^\circ - 34^\circ\text{N}$ ) is a rainy season called Meiyu. Precipitation increases from early July to mid-August over the Yellow River basin. Hereafter, we treat this period (30 June to 18 August) as a rainy season. Figure 2 indicates the interannual variation in the total precipitation during the rainy season. The long-term trend shows a weak decrease ( $-0.17\text{mm/day}$  per decade), but it is not statistically significant. This result is consistent with that of Endo et al.(2005). Meanwhile, there is a large interannual variation of  $\sim 100\text{mm}$  in amplitude. This is a significant variation because the climatological annual total precipitation is  $\sim 450\text{mm}$ . The interannual time series in the rainy season has significant correlation with that in the annual

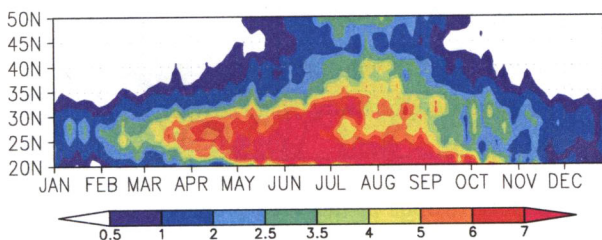


Fig.1: Time-latitude section in 25-year averaged precipitation (Xie et al. 2007) between  $105^\circ$  to  $120^\circ\text{E}$ . A unit is mm/day.

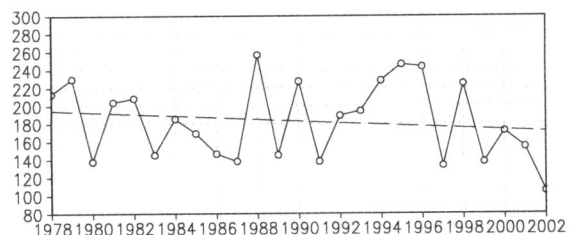


Fig. 2: Time series in the total precipitation (Xie et al., 2007) in the rainy season over the Yellow River basin (solid line with open square) and its linear trend (dashed line). A unit for the vertical axis is mm/50day.

total precipitation (about 0.7), suggesting that precipitation variation in the rainy season strongly affects the interannual variation in the annual total precipitation.

Next, precipitation variability in a larger area, associated with the interannual variation in rainy-season total precipitation over the Yellow River basin, is examined using GPCP data (Correlation between the interannual time series of the gauge-based precipitation and GPCP is 0.96 during 1979 – 2002).

Figure 3 shows the spatial distribution in the correlation coefficient between the interannual precipitation variation over the Yellow River basin and that in every grid point. Statistical significant positive correlations (shown as red shadings) extend from the Yellow River basin to western arid regions along 40°N, whereas significant negative correlations appear from the Yangtze River basin to the Korean Peninsula. Positive correlation is also observed over the western India. Figure 4 shows composites of precipitation distribution in wet years (1979, 1988, 1990, 1995 and 1998) and dry years (1980, 1991, 1997, 1999, and 2002), based on the time series in the Yellow River basin (Fig. 2). In the wet years, high precipitation area is observed centered around the Yellow River basin, while there is less precipitation areas from central China to the East China Sea (Fig4-left). In the dry years, high precipitation areas extend from southern China to the Korean Peninsula (Fig. 4-right).

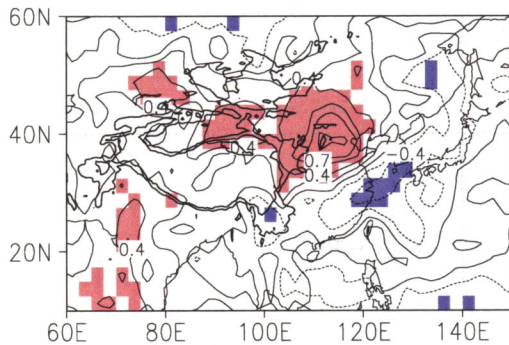


Fig.3: Correlation coefficients between the interannual variation in the rainy-season total precipitation over the Yellow River basin and that in every grid. Red (blue) shadings denote areas of positive (negative) correlation > 95 % confidence level. The 1,500 m and 3,000 m topographic contours are shown as thick solid lines.

1999 and 2002), based on the time series in the Yellow River basin (Fig. 2). In the wet years, high precipitation area is observed centered around the Yellow River basin, while there is less precipitation areas from central China to the East China Sea (Fig4-left). In the dry years, high precipitation areas extend from southern China to the Korean Peninsula (Fig. 4-right).

Using the time series in precipitation shown in Fig.2, atmospheric factors causing the interannual variation around the Yellow River basin are investigated by calculating regression patterns of meteorological fields in the rainy season. In the upper troposphere (200hPa; ~12000m), a wavetrain pattern (alternative distribution of cyclonic and anti-cyclonic anomalies) is remarkable to the east of 40°E along 40°N (Fig. 5-upper). Associated with the wavetrain, there are an anticyclonic anomaly centered on 40°N, 120°E and a cyclonic anomaly to its west. In middle to lower troposphere (500hPa; ~5500m and 850hPa; ~1500m), there is an anticyclonic circulation near

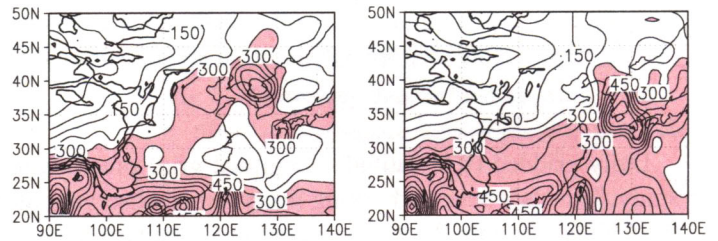


Fig. 4: Composites of precipitation distribution in wet years (left; 1979, 1988, 1990, 1995 and 1998) and dry years (right; 1980, 1991, 1997, 1999 and 2002). The contour interval is 50mm. Shading denotes areas with precipitation > 250mm.

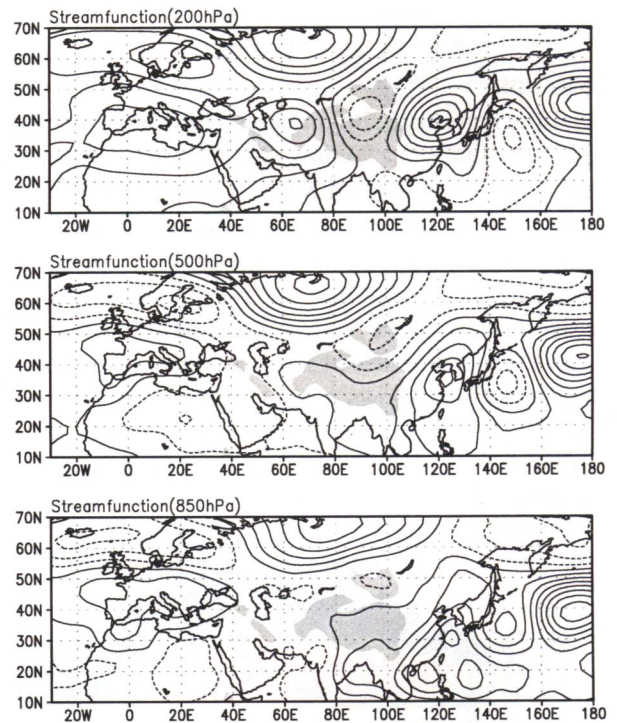


Fig. 5: Regressions of the streamfunction at (upper) 200 hPa, (middle) 500hPa and (bottom) 850 hPa in the rainy season for 1979 – 2006 to the timeseries in rainy-season precipitation over the Yellow River basin (Fig. 2). A positive (negative) value indicates anti-cyclonic (cyclonic) anomalies. Shading denotes areas > 1500m above sea level.

40°N, 120°E, similar to the location at 200 hPa. Therefore, the waves are nearly barotropic. The wavetrain is interpreted as a quasi-stationary Rossby wave propagating eastward along the Asian subtropical jet (Iwao and Sato 2006, Ding and Wang 2005). Pacific-Japan pattern (so-called PJ pattern), which is induced by convection anomalies over the western Pacific, is a major agent for forming large-scale circulation anomalies around East Asia (Nitta 1987). The PJ pattern is important for the interannual variation of summertime precipitation over the Yangtze River basin. However, the PJ-like pattern can not be observed in Figure 5, indicating that the interannual variation over the Yellow River basin is strongly affected by the eastward propagating stationary waves, rather than the PJ pattern.

The barotropic circulation structure around the Yellow River basin plays an important role in a moisture transport toward the basin. Figure 6 indicates regressions of moisture flux vector and its divergence. The anticyclonic circulation anomaly over the lower reaches of the basin induces the increase of southerly moisture flux into the basin at its southern boundary. The cyclonic anomaly, located to the east of the anticyclonic anomaly, also increase moisture flux crossing into the western boundary of the basin. Both the enhanced southerly and westerly fluxes results in the increase of precipitation over the Yellow River basin.

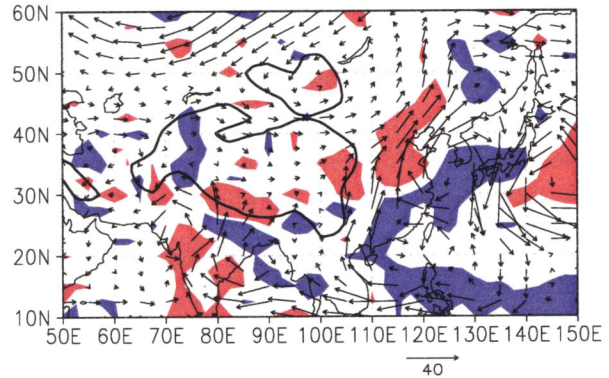


Fig.6: Regressions of moisture flux (vectors) and its divergence (shading) in the rainy season for 1979 – 2006 to the time series in rainy-season precipitation over the Yellow River basin (Fig. 2). Red (blue) shading denotes areas of convergence (divergence) anomaly.

### 3.2. Intraseasonal variation in precipitation over the Yellow River basin during the summer

In the rainy season, the precipitation time series shows alternatively active phase and inactive phase on 10 – 60 day timescales. The phenomenon is referred to as an intraseasonal variation. Figure 7 shows the timeseries in a wet-year (1988) summer precipitation over the Yellow River basin and its wavelet power spectrum. Precipitation increases in early July and then intraseasonal variation on ~14-day period becomes prominent (Fig.7-upper). ~3-day variation is also observed, probably associated with eastward migratory disturbances. Precipitation decreases again after mid-August. Interestingly, the amplitude of ~3-day variation is modulated on ~14-day period. In a dry year of 1997, ~14-day period was also dominant during the summer. This suggests that the period of intraseasonal variation is not necessarily associated with the interannual variation of rainy-season total precipitation.

The intraseasonal variation in precipitation over the Yellow River basin is induced by that in quasi-stationary waves along the Asian subtropical jet. Rainy-season mean circulation fields are provided by the modulation of the activity of the intraseasonal variation. Figure 8 shows the time-longitude section in a 200-hPa meridional wind component along 40° N in 1988 summer. An active (inactive) phase in precipitation over the Yellow River basin (105° –

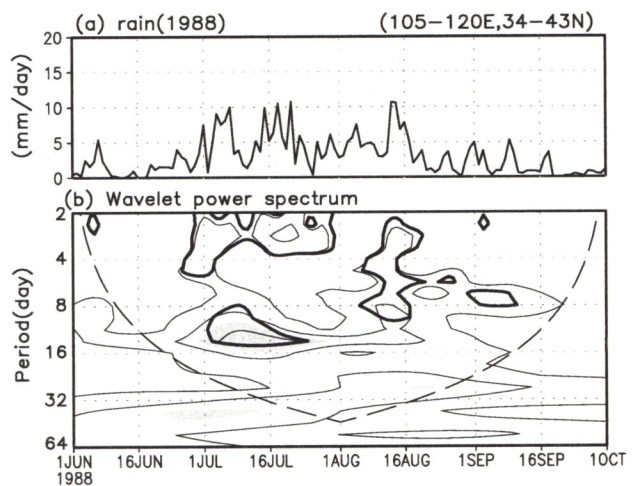


Fig. 7 : Timeseries in summertime precipitation of 1988 (upper) and its wavelet power spectrum (bottom). The thick solid (dotted) contour line encloses regions of > 95% confidence for a red-noise process with a lag-1 coefficient.

120° E) corresponds to a southerly (northerly) phase at the upper troposphere. The alternation between southerly and northerly winds over the Yellow River basin causes the large amplitude precipitation fluctuation. A large circulation fields causing the meridional wind variation has a barotropic structure as well as the interannual variation as shown in Fig. 5. Thus, southerly (northerly) winds import moist (dry) air masses over the Yangtze River basin and cause the increase of convective activity there. The rainy-season mean value in meridional wind of 1988 shows positive (i.e. southerly wind) over the Yellow River basin. This is consistent with wind fields induced by circulation anomalies shown in Fig.5-upper. In 1997, intraseasonal variation in a meridional wind was also remarkable over the Yellow River basin as well (not shown). However, 1997 summer had a longer spell of dry phase than 1998 summer did because northerly wind last for a longer time. The rainy-season mean meridional wind showed negative value (i.e. northerly wind) over the Yellow River basin in 1997. In short, the interannual variation in the rainy-season total precipitation over the Yellow River basin depends on the meridional wind variation induced by intraseasonal variation of waves in the upper troposphere. Whether the upper-level waves induce northerly or southerly over the Yellow River basin depend on the location of wave generation, wave length, periodicity of intraseasonal variation and so on. Further studies will be needed to understand what process determines them.

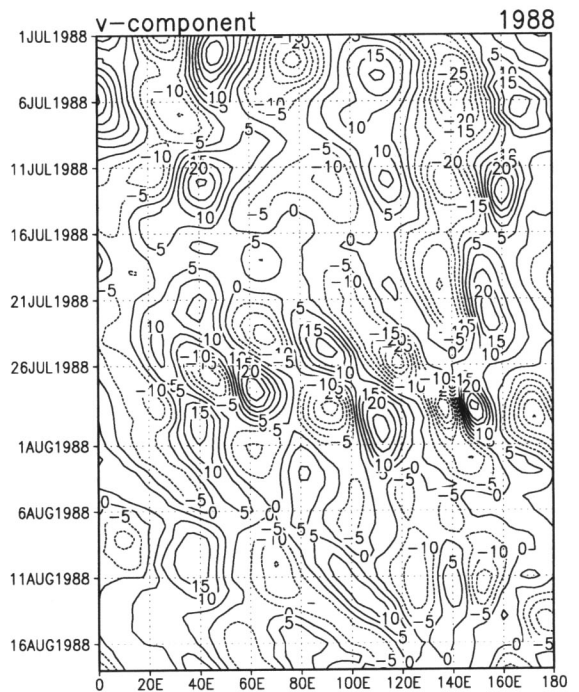


Fig. 8: Time-longitude section in 200-hPa meridional wind in 1988 along 40°N. Positive (negative) value indicates a southerly (northerly) wind.

## References

- Ding, Q. and B. Wang, 2005: Circumglobal Teleconnection in the Northern Hemisphere Summer, *J. Climate*, **18**, 3483-3505.
- Endo, N, Ailikun, B. and T. Yasunari, 2005: Trends in precipitation amounts and the number of rainy days and heavy rainfall events during summer in China from 1961 to 2000, *J. Meteor. Soc. Japan*, **83**, 621-631.
- Huffman, G. J. and Coauthors, 1997: The global precipitation climatology project (GPCP) combined precipitation dataset, *Bull. Amer. Meteor. Soc.*, **78**, 5-20.
- Iwao, K., and M. Takahashi, 2006: Interannual change in summertime precipitation over northeast Asia, *Geophys. Res.Lett.*, **33**, L16703, doi:10.1029/2006GL 027119.
- Kalnay, E, and Coauthors, 1996: The NCEP/NCAR 40-Year reanalysis project, *Bull. Amer. Meteor. Soc.*, **77**, 437-471.
- Nitta, T. 1987: Convective activities in the tropical western Pacific and their impact on the northern hemisphere summer circulation, *J. Meteor. Soc. Japan*, **65**, 373-390.
- Xie, P. and Coauthors, 2007: A Gauge-Based Analysis of Daily Precipitation over East Asia, *J. Hydrometeor.*, **8**, 607-626.
- Yatagai, A and T. Yasunari, 1995: Interannual variations of summer precipitation in the arid/semi-arid regions in China and Mongolia: their regionality and relation to the Asian summer monsoon, *J. Meteor. Soc. Japan*, **73**, 909-923.